Acta Crystallographica Section D
Biological Crystallography
ISSN 0907-4449

Structure of oxalate-substituted diferric mare lactoferrin at 2.7 Å resolution

Ashwani K. Sharma and Tej P. Singh*

Department of Biophysics, All India Institute of Medical Sciences, New Delhi 110 029, India

Correspondence e-mail: tps@medinst.ernet.in

Received 28 May 1999
Accepted 29 June 1999

PDB Reference: oxalate-substituted diferric mare lactoferrin, 1b7z.

Lactoferrin binds two Fe^{3+} and two CO_3^{2-} ions with high affinity. It can also bind other metal ions and anions. In order to determine the perturbations in the environments of the binding sites in the N and C lobes and elsewhere in the protein, the crystal structure of oxalate-substituted diferric mare lactoferrin has been determined at 2.7 Å resolution. The final model has a crystallographic R factor of 21.3% for all data in the resolution range 17.0–2.7 Å. The substitution of an oxalate anion does not perturb the overall structure of the protein, but produces several significant changes at the metal-binding and anion-binding sites. The binding of the oxalate anion is symmetrical in both the N and C lobes, unlike in diferric dioxalate human lactoferrin, where the oxalate anion binds the metal ion symmetrically in the C lobe and asymmetrically in the N lobe.

1. Introduction

Lactoferrin is an iron-binding protein (Aisen & Listowsky, 1980; Brock, 1985) which serves to control the iron levels in body fluids by sequestering and solubilizing ferric ion. It has many other functions such as antibacterial (Arnold *et al.*, 1977) and growth-factor activities (Berseth *et al.*, 1983). It is also found in white blood cells and secretory fluids (milk, tears, saliva *etc.*; Mason *et al.*, 1969; Mason & Heremans, 1971; Biserte *et al.*, 1963; Sthuchell *et al.*, 1981) and as a modulator of the immune and inflammatory responses (Leffel & Spitznagel, 1975). So far, the best understood and most characteristic feature of lactoferrin proteins is their ability to bind very tightly ($K \simeq 1020$) but reversibly two Fe^{3+} ions together with two CO_3^{2-} ions in a unique synergistic relationship between metal and anion binding. The carbonate ion binds to the Fe atom in a bidentate mode (Haridas *et al.*, 1995; Sharma, Paramasivam *et al.*, 1999). It also forms hydrogen bonds with residues of domain 2 in each lobe. The structural role of carbonate ion is to neutralize the positive charge presented by an essential arginine side chain and the N terminus of helix 5 and to fill two *cis* coordination positions of the Fe^{3+} ion. In mare lactoferrin, the carbonate ion was not found to interact with Fe^{3+} in a symmetrical fashion (Sharma, Paramasivam *et al.*, 1999). The basis of this asymmetry was not clear. Therefore, it was necessary to study the structure of mare lactoferrin with other ions to determine the relative strengths of interactions of various anions. Although Fe^{3+} and CO_3^{2-} appeared to be the preferred species bound to the protein and are probably of the greatest physiological significance, many other metal ions (Haridas *et al.*, 1995; Smith *et al.*, 1992; Sharma, Kumar *et al.*, 1999; Sharma, Paramasivam *et al.*, 1999; Sharma & Singh, 1999; Moore *et al.*, 1997; Karthikeyan *et al.*, 1999) and anions (Smith *et al.*, 1992; Baker *et al.*, 1996) can also bind,

Table 1
Summary of the crystallographic data.

Space group	$P2_12_12_1$
Unit-cell parameters (Å)	a = 84.5, b = 99.8, c = 103.9
V_m (Å^3 Da^{-1})	2.72
Calculated solvent content (%)	54.8
Resolution range (Å)	17.0–2.7
Total number of reflections measured	126098
Total number of unique observed reflections	21691
Average $I/\sigma(I)$	18.0
R_{sym} (%)	12
Completeness (%)	90
Completeness in the outer resolution shell (2.8–2.7 Å) (%)	81
Solvent content (%)	55
Z (number of molecules in the unit cell)	4

apparently in the same sites (Gerstein *et al.*, 1992). Other anions, most of them carboxylate ions (oxalate, malonate, glycolate *etc.*), can substitute for carbonate under carbonate-free conditions. The question of how these varying anions are bound and the extent to which they perturb the protein structure is of fundamental importance in understanding their physiological significance.

The second question is regarding the equivalence of the two sites. Although the sites in the N and C lobes appear to be essentially identical, detailed crystallographic studies in mare lactoferrin have shown that the bindings of Fe^{3+} and CO_3^{2-} are more symmetrical in the N lobe than in the C lobe, while the reverse was observed in human lactoferrin. The origin of these inequivalences in a single protein and between proteins of different species is not yet clearly known.

The physiological significance of iron binding and the prevalence of different metabolites such as carbonate, oxalate, glycolate *etc.* which can act as synergistic anions needs to be understood. It is also important to study the combinations of various metal ions and anions complexed with lactoferrin. Such studies will provide a clear picture of protein–cation, protein–anion, cation–anion and protein–cation–anion associations. Also, the significance of these combinations in different species needs to be determined. Therefore, we present here the crystal structure of a complex of mare lactoferrin in which oxalate is used as the synergistic anion with Fe^{3+} as the associated cation. The present studies on the complex of diferric dioxalate lactoferrin [$Fe_2(C_2O_4)_2$Lf] show how the larger oxalate anion is accommodated in the binding cleft without major disturbances in the overall polypeptide structure.

2. Experimental

2.1. Preparation of diferric dioxalate lactoferrin [$Fe_2(C_2O_4)_2$Lf]

Mare apolactoferrin, prepared from fresh samples of colostrum, was used for preparation of the oxalate complex in a carbonate-free environment. Sodium oxalate was added in excess (50-fold molar excess) to a solution of apolactoferrin (30 mg ml^{-1}) in 50 mM Tris–HCl pH 8.0 containing 0.1 M NaCl. Ferric chloride reagent was then added to the solution. The resulting complex was purple–red in color, with a visible absorption maximum at 482 nm, whereas the carbonate complex is orange–red in colour with a visible absorption maximum at 465 nm.

2.2. Crystallization of the protein

The complex was immediately used for crystallization using the microdialysis method. Crystals suitable for X-ray diffraction were obtained with protein solutions of concentration ranging from 20–30 mg ml^{-1} in 0.025 M Tris–HCl dialyzed against the same buffer brought to 10%(v/v) ethanol at pH 8.5. The crystallization experiments were carried out at 279 K. The purple–red crystals grew in two weeks to dimensions 0.5 × 0.3 × 0.2 mm.

2.3. Data collection

Crystals were mounted in 0.7 mm diameter glass capillaries. X-ray intensities were measured at 288 K using a MAR Research imaging-plate scanner with a diameter of 300 mm; the crystal-to-detector distance was 230 mm. Monochromatic Cu $K\alpha$ radiation was produced with a graphite-crystal monochromator mounted on a Rigaku RU-200 rotating-anode generator operating at 40 kV and 100 mA with a focal point of 0.3 × 3 mm. 100 images with 1° rotation were collected. The exposure time was 10 min per image. The complete data set was obtained using one crystal. The crystals diffracted well to 2.7 Å resolution.

2.4. Data processing

The *HKL* (Otwinowski, 1993; Minor, 1993), *MARXDS* and *MARSCALE* (Kabsch, 1988) packages were used for the determination of unit-cell parameters, data processing and scaling. The crystals belonged to the orthorhombic system, space group $P2_12_12_1$, with one molecule in the asymmetric unit. The unit-cell dimensions were found to be a = 84.5, b = 99.8, c = 103.9 Å with a solvent content of 55%. These crystals were isomorphous to those of $Fe_2(CO_3)_2$ lactoferrin (a = 85.2, b = 99.5, c = 103.1 Å). The data were complete to 90% with 21691 unique reflections in the resolution range 17.0–2.7 Å. R_{sym} was found to be 0.12. The details of the crystallographic data-collection and processing statistics are given in Table 1.

2.5. Structure determination and refinement

The crystals of $Fe_2(C_2O_4)_2$Lf were isomorphous with those of native diferric lactoferrin [$Fe_2(CO_3)_2$Lf]. Therefore, the refined atomic coordinates of diferric lactoferrin structure were used as the starting model for refinement, after removing Fe^{3+} and CO_3^{2-} ions, the solvent molecules, protein side chains involved in metal binding (four in each binding site) and anion-binding protein side chains (Arg121, Arg463, Thr117 and Thr459). All of these protein side chains were mutated to alanine. The individual temperature factors were given an initial value of 25 Å^2. The model was refined against 21691 reflections in the resolution range 17.0–2.7 Å without any σ cutoff. The initial R value was 0.37. The model was refined

Table 2
Details of the refinement of the structure.

Resolution limits (Å)	17.0–2.7
Number of reflections	21691
Final R factor (all data %)	21.3
R_{free} (3% of data)	27.4
Number of protein atoms	5281
Number of solvent molecules	70
Ions	2 Fe^{3+}, 2 $C_2O_4^{2-}$
Average B value (Å^2)	
For all atoms	39.7
R.m.s. deviation for B factors	3.2
For main-chain atoms	37.7
For side-chain atoms	41.7
R.m.s. deviations from ideal values	
Bond lengths (Å)	0.013
Bond angles (°)	2.0
Dihedral angles (°)	23.7
Improper angles (°)	2.1
Ramachandran plot (non-Gly, non-Pro)	
Residues in most allowed regions (%)	80.5
Residues in additionally allowed regions (%)	17.4
Residues in generously allowed regions (%)	1.8
Residues in disallowed regions† (%)	0.3

† Leu299 and Leu640 were present in disallowed regions. These are the central residues of two conserved γ-turns in lactoferrins.

using the program *X-PLOR* (Brünger *et al.*, 1987) followed by manual rebuilding with the program *O* (Jones *et al.*, 1991). The refinement protocol in *X-PLOR* consisted of rigid-body refinement (40 cycles using the 17.0–4.0 Å data) followed by simulated annealing (17.0–2.7 Å), a conventional positional refinement (50 cycles, 17.–2.7 Å) and B-factor refinement (20 cycles, 17.0–2.7 Å). A randomly chosen 3% of the reflections in the data set were used for R_{free} calculations. The rigid-body refinement was carried out taking the N lobe and C lobe as two separate rigid bodies, residues 1–344 (N-terminal lobe) and 345–689 (C-terminal lobe). Many cycles of refinement and model building using 'positional' and 'prepstage' in the *X-PLOR* protocol were performed. The Fe^{3+} and metal ligands were added to the model when the R value was 28%. After a further ten cycles of refinement, the R factor dropped to 26%. At this stage, inspection of $2F_o - F_c$ and $F_o - F_c$ maps clearly showed the electron density for the anion as well as for the two side chains which interact with the anion. The anion density appeared to be bilobal in nature at both sites (Fig. 1). The two oxalate ions and their associated protein side chains (Thr117 and Arg121 in the N-lobe, Thr459 and Arg463 in the C lobe) were added to the model. The oxalate ion, bound in a 1,2-bidentate fashion, was found to fit almost perfectly in the available density. The omit map calculated for the oxalate anion clearly indicated the bidentate orientation for the oxalate. Water molecules were added to the model when the R factor was below 25%, where the difference density had values of more than 3σ above the mean and the $2F_o - F_c$ map showed density at more than 1σ level, and each water molecule had at least one interaction with protein or other solvent molecules. Individual B factors were refined for all atoms. The final R factor was 0.213 for all data in the resolution range 17.0–2.7 Å. The final refinement statistics are given in Table 2.

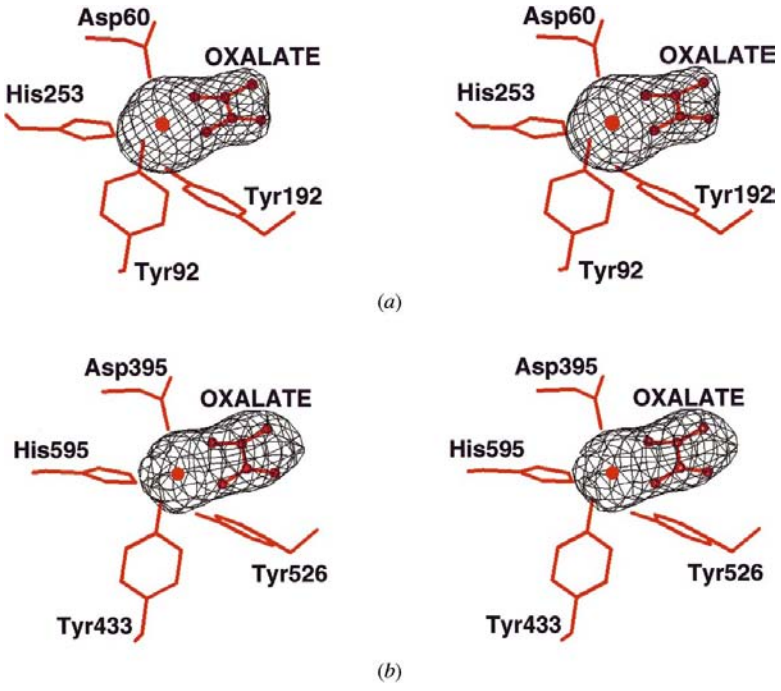

Figure 1
(*a*) The N-lobe iron-binding site and (*b*) the C-lobe iron-binding site of mare lactoferrin showing $F_o - F_c$ electron density (contoured at the 3.0σ level).

3. Results

3.1. The final model

The set of final atomic coordinates comprises 5281 protein atoms (from 689 amino-acid residues), two Fe^{3+} ions, two $C_2O_4^{2-}$ ions and 70 solvent molecules. The protein structure has a geometry which is close to ideal, with r.m.s. deviations of 0.013 Å and 2.0° from standard values of the bond lengths and bond angles, respectively. The final crystallographic R factor was 0.213 for all 21691 reflections in the 17.0–2.7 Å resolution range. The protein chain folds into two globular N and C lobes which contain N1, N2 and C1, C2 domains, respectively (Fig. 2).

A Luzzati plot (Luzzati, 1952) of the R factor as a function of resolution gave a value of 0.24 Å for the mean absolute error in atomic positions, while a σ_A plot (Read, 1986) indicated a value of 0.31 Å. The error is probably less in well defined regions of the structure but is substantially higher in some poorly defined regions of the molecule such as loops on the surface of the protein. This may also be a consequence of the inclusion of weak reflections from the higher resolution shells in the refinement. The distribution of main-chain torsion angles (Ramachandran & Sasisekaran, 1968) was calculated using the program *PROCHECK* (Laskowski *et al.*, 1993). The most favoured regions account for 80.5% of the non-glycine residues, while a further 17.4% of residues occupy the additionally allowed regions and 1.8% are in generously allowed regions. Only two

residues, Leu299 and Leu640, were present in disallowed regions. These are the central residues of two γ-turns which are in equivalent positions in the N and C lobes. Their (γ, ψ) values are around (70, -50°), which are very similar to the characteristic values for classic γ-turns (Matthews, 1972; Nemethy & Printz, 1972) which are around (70, -50°) (Baker & Hubbard, 1984). These two γ-turns are located in part of one wall of the binding cleft of each lobe, and their highly conserved sequence of Leu–Leu–Phe seems likely to be a common feature of the structures of the family of transferrin proteins. These γ-turns are in equivalent positions in the N and C lobes of the protein.

The mean B value for all protein atoms is 39.7 Å^2. The distribution of B values along the polypeptide chain follows the expected pattern, with secondary structures and internal regions having lower values and external loops much higher values. The metal-binding and anion-binding sites have relatively low B values. The regions with high B values are mostly external loops connecting the secondary-structure elements. Here, the structure is flexible because of the hydrogen bonding to solvent molecules only and is, therefore, not well defined. B values are also higher for some helices which are present on the surface (helix 1 at the C-terminal end).

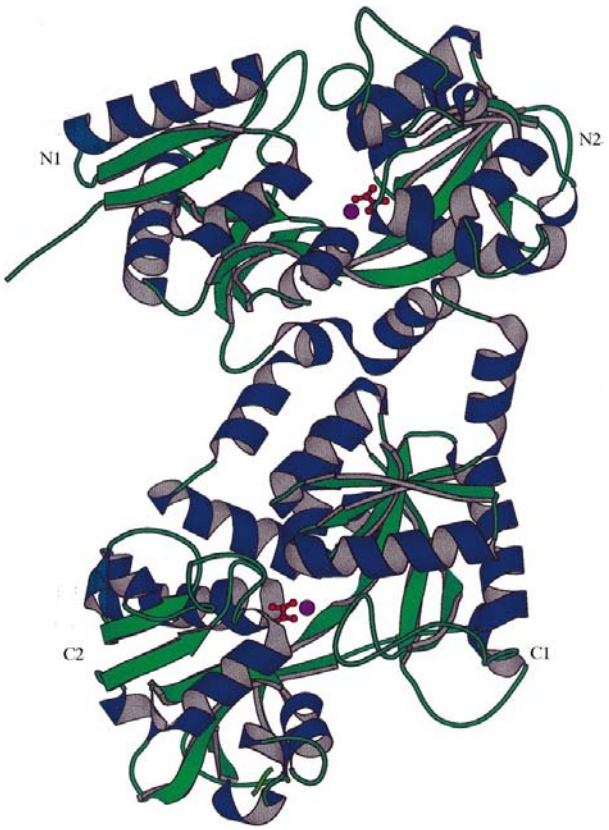

Figure 2
Schematic diagram of diferric dioxalate mare lactoferrin showing the arrangements of two lobes and four domains in the protein. The figure also shows the positions of Fe^{3+} and the oxalate ions. The figure was drawn using *BOBSCRIPT* (Esnouf, 1997).

3.2. Polypeptide folding

The polypeptide-chain folding of $Fe_2(C_2O_4)_2$Lf is closely similar to that of dicarbonate diferric lactoferrin. There are no major conformational differences between the two structures except at the metal-binding and anion-binding sites. The superposition of the $Fe_2(C_2O_4)_2$Lf structure onto the $Fe_2(CO_3)_2$Lf shows that the whole molecule superimposes with a root-mean-square deviation of 0.28 Å (689 C^α atoms). The superimposition of individual lobes and domains of the two structures gave root-mean-square deviations which confirmed the similarities in their folding: N lobe, 0.20 Å (334 C^α atoms), 0.31 Å (for all atoms); C lobe, 0.19 Å (345 C^α atoms), 0.36 Å (for all atoms); N1 domain, 0.19 Å (172 C^α atoms), 0.28 Å (for all atoms); N2 domain, 0.21 Å (161 C^α atoms), 0.34 Å (for all atoms); C1 domain, 0.17 Å (183 C^α atoms), 0.38 Å (for all atoms); C2 domain, 0.21 Å (162 C^α atoms), 0.33 Å (for all atoms). If the C lobes of $Fe_2(CO_3)_2$Lf and $Fe_2(C_2O_4)_2$Lf are superimposed, then a rotation of 1.2° is required to bring the two N lobes into coincidence. The comparison of individual domains of each lobe for the closure over metal and anion sites shows that if the N2 domains of $Fe_2(C_2O_4)_2$Lf and $Fe_2(CO_3)_2$Lf are superimposed, a rotation of 0.3° is required to bring the two N1 domains into coincidence. Similarly, if the C2 domains are superimposed on each other, a rotation of 0.4° is needed to bring the two C1 domains into coincidence.

3.3. The metal and anion sites

In both the N- and C-lobe binding sites, the oxalate ion is bound to the Fe^{3+} ion in 1,2-bidentate mode (Fig. 3). The coordination distances to Fe^{3+} are listed in Table 3(*a*), while the anion hydrogen-bonding distances are listed in Table 3(*b*). The Fe atom has shifted slightly (0.2 Å in N lobe and 0.3 Å in C lobe) relative to the native diferric dicarbonate lactoferrin structure. The four protein ligands occupy almost identical positions (shifts <0.3 Å). The larger size of the oxalate anion compared with the carbonate anion was expected to cause significant displacements of the arginine side chain from its position in $Fe_2(CO_3)_2$Lf. The observed average movement of the guanidinium group in both lobes is of the order of 0.4–0.5 Å. The displacement is restricted owing to the involvement of arginine in various interactions with neighbouring residues. In the N lobe, Arg121 NH1 interacts with the aromatic ring of Phe190, while in the C lobe, Arg463 NH1 is strongly hydrogen bonded to Tyr524 OH at a distance of 2.57 Å. The corresponding hydrogen-bonding distance in $Fe_2(CO_3)_2$Lf is 2.94 Å.

The oxalate anion makes a series of hydrogen bonds with the residues of the anion-binding site from domain 2 of each lobe. The hydrogen-bonding pattern is similar in both sites (Fig. 3). The carboxylate groups of oxalate form hydrogen bonds with the peptide NH groups of helix 5, the side-chain OH of Thr117 (459) and Arg121 (463).

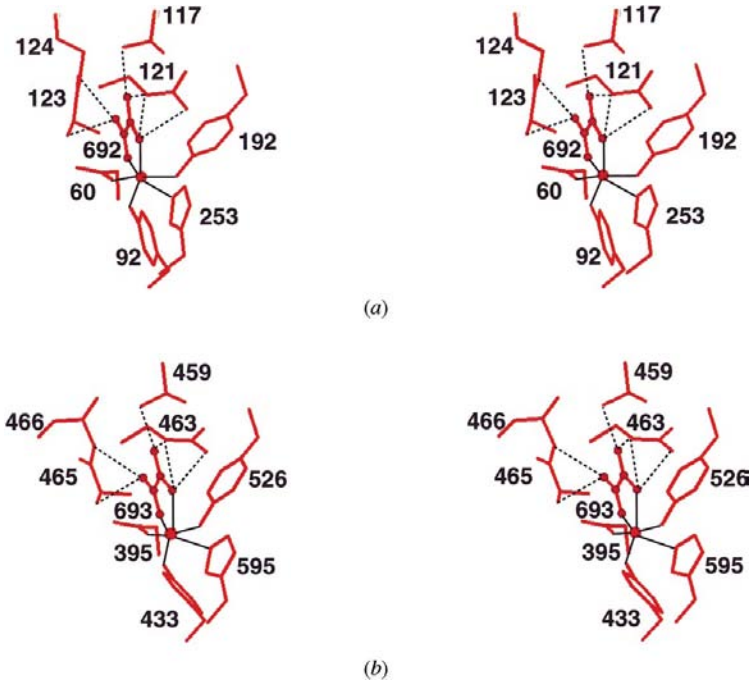

Figure 3
The coordination of metal ion and anion (oxalate) with the protein in (*a*) the N lobe and (*b*) the C lobe.

4. Discussion

The structure of oxalate-substituted diferric mare lactoferrin shows that binding of the larger oxalate ion in place of carbonate anion does not significantly perturb the protein conformation. The oxalate ion was synergistically bound and it was able to induce the same environment as occurs with the physiologically important carbonate ion. The only significant differences were found in the vicinity of the metal-binding and anion-binding sites (Fig. 4).

In both sites, the oxalate anions coordinate to the metal ions in a 1,2-bidentate mode to give rise to a distorted octahedral geometry. The anion binding is found to be symmetrical in both the N and C lobes, with the metal being at almost equal distances from both the coordinating O atoms of the oxalate anions. The substitution of a larger anion such as oxalate in both sites requires only a slight displacement of the arginine side chain. This displacement, however, does not prevent hydrogen bonding between the arginine guanidinium group and the anion. In both sites, the interactions of arginine with residues in the vicinity play an important role in the displacement. In the N lobe, the displacement of Arg121 is restricted by the

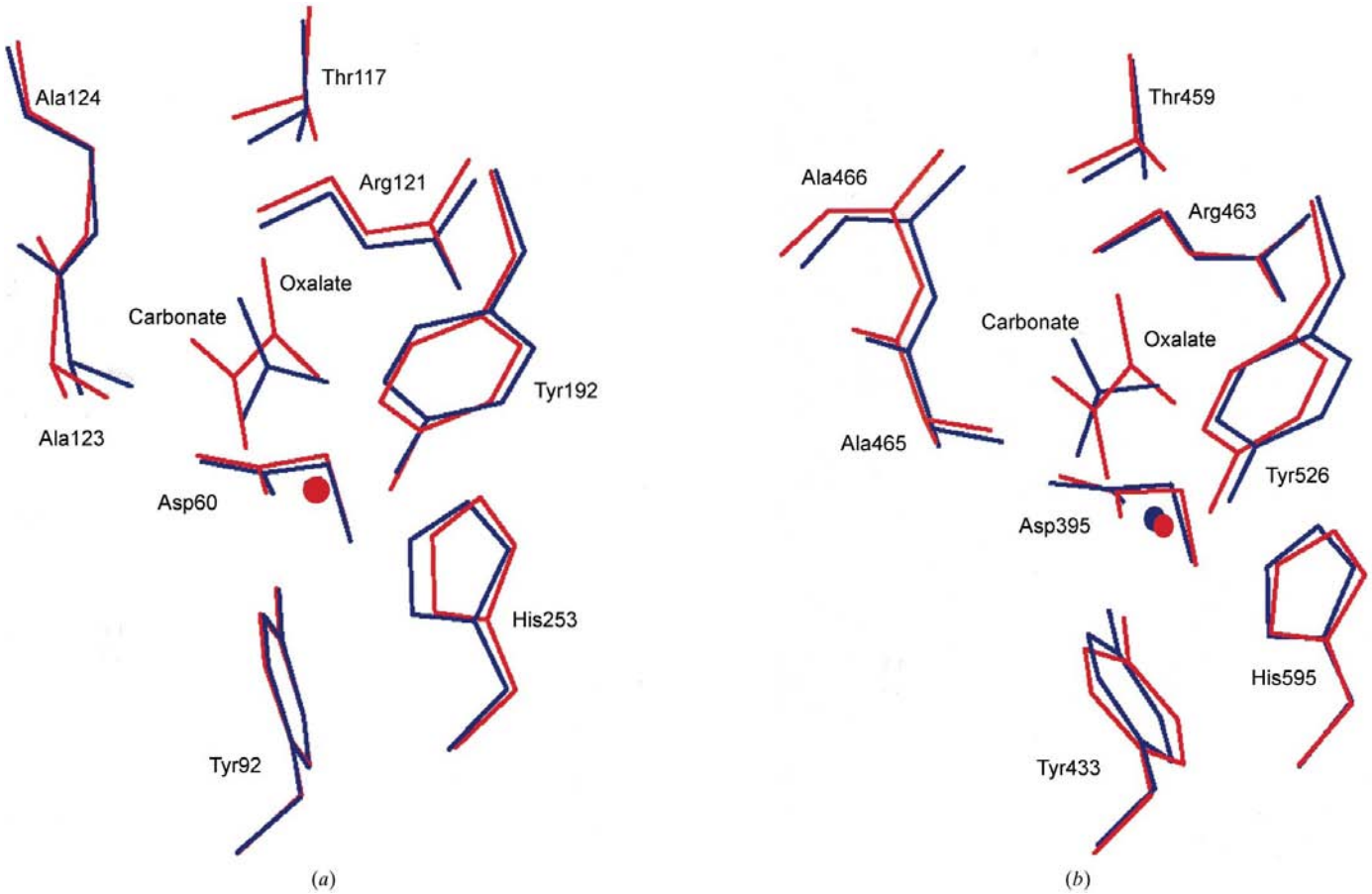

Figure 4
Superposition of the metal-ion coordination site in (*a*) N lobes and (*b*) C lobes of diferric dioxalate lactoferrin (red) and diferric dicarbonate lactoferrin (blue).

Table 3
Metal coordination and anion hydrogen-bonding distances.

(*a*) Coordination distances in metal and anion sites

N lobe		C lobe	
Atoms	Bond length (Å)	Atoms	Bond length (Å)
Fe—O Asp60	2.0	Fe—O Asp395	1.9
Fe—O Tyr92	1.9	Fe—O Tyr433	2.0
Fe—O Tyr192	1.9	Fe—O Tyr526	2.0
Fe—N His253	2.5	Fe—N His595	2.4
Fe—O1 oxalate	1.9	Fe—O1 oxalate	1.9
Fe—O2 oxalate	2.0	Fe—O2 oxalate	2.2

(*b*) Anion hydrogen-bonding distances in the two lobes

N lobe		C lobe	
Hydrogen bond	Bond length (Å)	Hydrogen bond	Bond length (Å)
O2···NH2 (121)	3.1	O2···NH2 (463)	2.8
O2···NE (121)	3.0	O2···NE (463)	3.2
O3···N (123)	2.6	O3···N (465)	2.6
O3···N (124)	2.7	O3···N (466)	3.0
O4···OG1 (117)	2.6	O4···OG1 (459)	2.6
O4···NE (121)	2.8	O4···NE (463)	2.8

presence of Phe190 and the distance between NH1 and phenyl ring is 3.4 Å, whereas in the case of the carbonate anion the distance is 3.6 Å. Similarly, in the C lobe Arg463 forms a hydrogen bond with Tyr524 OH at a distance of 2.57 Å, while

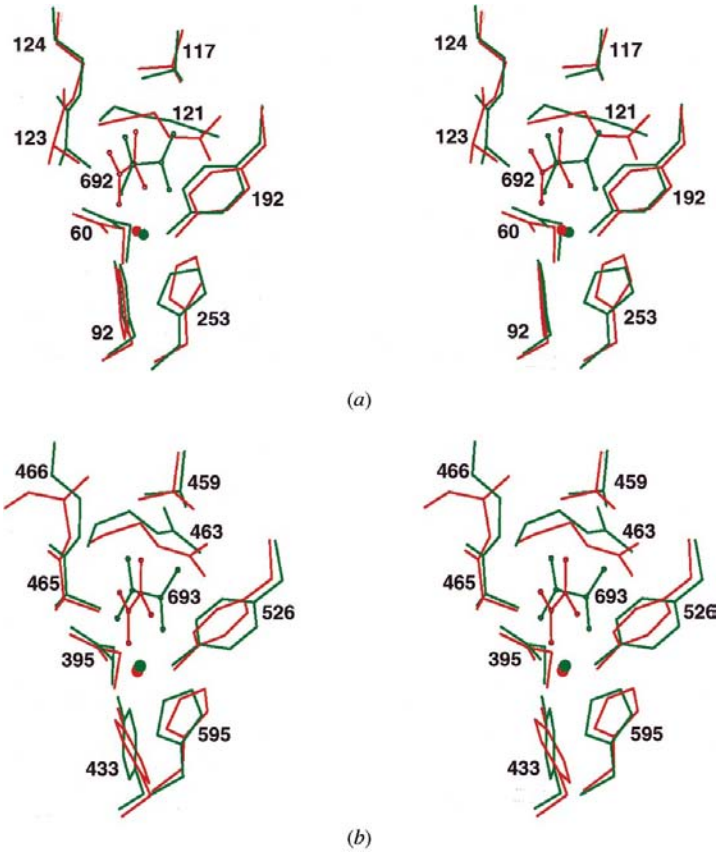

Figure 5
Superposition of iron-binding sites in (*a*) the N lobe and (*b*) the C lobe of human (red) and mare (green) lactoferrins.

Table 4
Comparison of oxalate and carbonate anion coordination distances between mare and human lactoferrins.

	Mare lactoferrin		Human lactoferrin	
	N lobe	C lobe	N lobe	C lobe
Carbonate distances				
Fe—O1	2.0	1.9	2.1	2.1
Fe—O2	1.9	2.5	2.2	2.1
Oxalate distances				
Fe—O1	1.9	1.9	1.9	1.9
Fe—O2	2.0	2.2	2.6	2.1

the corresponding distance in the carbonate-substituted lactoferrin is 2.94 Å. This interaction restricts larger movements of the arginine side chain. It indicates that both the carbonate and oxalate anions can be accommodated without much perturbation of the protein structure. In fact, the observed interactions of lactoferrin with oxalate seem to be quite favourable. Therefore, it is expected that other dicarboxylate anions such as malonate will also bind in a similar manner to oxalate.

On comparing the present structure with the other oxalate-substituted lactoferrin structures, such as the $Fe_2(C_2O_4)_2$ human lactoferrin structure (Baker *et al.*, 1996), it has been found that significant changes occur only at the metal-binding sites. In the $Fe_2(C_2O_4)_2$ human lactoferrin structure, the oxalate is bound to the metal ion in a symmetrical bidentate mode in the C lobe and the binding in the N lobe is considerably asymmetrical, while in the present structure the bidentate oxalate ion interacts in a symmetrical fashion in both lobes (Table 4). Furthermore, the interactions of oxalate anions in human lactoferrin indicate the formation of seven hydrogen bonds in the N lobe and only five hydrogen bonds in the C lobe, whereas in mare lactoferrin six hydrogen-bonded interactions are observed in both lobes. This observation suggests that the cation–anion binding sites are identical in both lobes of mare lactoferrin, whereas in human lactoferrin they differ considerably. The superpositions of the binding sites in human and mare lactoferrins are shown in Fig. 5. Similar observations were made in carbonate-substituted human and mare lactoferrins. Overall, the conformational changes caused by the introduction of oxalate in place of carbonate were not found to be very significant.

The crystal structures of diferric human lactoferrin (Anderson *et al.*, 1989; Haridas *et al.*, 1995), dicupric human lactoferrin (Smith *et al.*, 1992), diferric mare lactoferrin (Sharma, Paramasivam *et al.*, 1999), disamarium mare lactoferrin (Sharma & Singh, 1999) and dimanganese mare lactoferrin (Sharma, Kumar *et al.*, 1999) have revealed that major rearrangement only occurs at the two metal-binding sites, while the rest of the protein structure remains unaltered. These observations clearly indicate that the substitution of different cations and anions do not perturb the overall structure of the protein, as the local adjustments at the binding

sites provide enough scope to accommodate them. However, a complete removal of ions from the protein causes drastic changes in both lobes of duck ovotransferrin (Rawas *et al.*, 1997) and in the N lobe of human lactoferrin (Norris *et al.*, 1991), while in the case of mare lactoferrin (Sharma, Rajashankar *et al.*, 1999) the structures of both lobes remained unaltered. Thus, the structures of iron-free forms of lactoferrins might differ from species to species but their ion-saturated forms are very similar. The significance of species-dependent structures of apo-proteins is not yet understood, but it is clear that lactoferrin can accommodate different metal ions and various anions efficiently, thus indicating its wider sequestering capability.

The authors thank S. Karthikeyan for helpful discussions and Dr M. P. Yadav for the supply of mare colostrum. Financial assistance from the Department of Biotechnology (New Delhi) is greatfully acknowledged.

References

Aisen, P. & Listowsky, I. (1980). *Annu. Rev. Biochem.* **49**, 357–393.

Anderson, B. F., Baker, H. M., Norris, G. E., Rumball, S. V. & Baker, E. N. (1989). *J. Mol. Biol.* **209**, 711–734.

Arnold, R. R., Cole, M. F. & McGhee, J. R. (1977). *Science*, **197**, 263–265.

Baker, E. N. & Hubbard, R. E. (1984). *Prog. Biophys. Mol. Biol.* **44**, 97–179.

Baker, H. M., Anderson, B. F., Brodie, A. M., Shongwe, M. S., Smith, C. A. & Baker, E. N. (1996). *Biochemistry*, **35**, 9007–9013.

Berseth, C. L., Lichtenberger, L. M. & Morriss, F. H. (1983). *Am. J. Clin. Nutr.* **37**(1), 52–60.

Biserte, G., Havez, R. & Cuvelier, R. (1963). *Exp. Ann. Biochim. Med.* **24**, 85–120.

Brock, J. H. (1985). *Arch. Dis. Child.* **55**, 417–421.

Brünger, A. T., Kuriyan, J. & Karplus, M. (1987). *Science*, **235**, 458–460.

Esnouf, R. M. (1997). *J. Mol. Graph.* **15**, 132–134.

Gerstein, M., Anderson, B. F., Norris, G. E., Baker E. N., Lesk, A. M. & Harrington, J. P. (1992). *Int. J. Biochem.* **24**, 275–280.

Haridas, M., Anderson, B. F. & Baker, E. N. (1995). *Acta Cryst.* D**51**, 629–646.

Jones, T. A., Zou, J., Cowan, S. W. & Kjeldgaard, M. (1991). *Acta Cryst.* A**47**, 110–119.

Kabsch, W. (1988). *J. Appl. Cryst.* **21**, 916–924.

Karthikeyan, S., Yadav, S., Paramasivam, M., Srinivasan, A. & Singh, T. P. (1999). *Acta Cryst.* D**55**. Submitted.

Laskowski, R. A., MacArthur, M. W., Moss, D. S. & Thornton, J. M. (1993). *J. Appl. Cryst.* **26**, 283–291.

Leffel, M. S. & Spitznagel, J. K. (1975). *Infect. Immunol.* **12**, 813–820.

Luzzati, V. (1952). *Acta Cryst.* **5**, 802–810.

Mason, P. L. & Heremans, J. F. (1971). *Comput. Biochem. Physiol.* **39**B, 119–129.

Mason, P. L., Heremans, J. F. & Schonne, E. J. (1969). *J. Exp. Med.* **130**, 643–658.

Matthews, B. W. (1972). *Macromolecules*, **5**, 818–819.

Minor, W. (1993). *XDISPLAYF Program*, Purdue University.

Moore, S. A., Anderson, B. F., Groom, C. R., Haridas, M. & Baker, E. N. (1997). *J. Mol. Biol.* **274**, 222–236.

Nemethy, G. & Printz, M. P. (1972). *Macromolecules*, **5**, 755–758.

Norris, G. E., Anderson, B. F. & Baker, E. N. (1991). *Acta Cryst.* B**47**, 998–1004.

Otwinowski, Z. (1993). *Proceedings of the CCP4 Study Weekend. Data Collection and Processing*, edited by L. Sawyer, N. Isaacs & S. Bailey, pp. 56–62. Warrington: Daresbury Laboratory.

Ramachandran, G. N. & Sasisekaran, V. (1968). *Adv. Prot. Chem.* **23**, 283–438.

Rawas, A., Muirhead, A. & Williams, J. (1997). *Acta Cryst.* D**53**, 464–468.

Read, R. J. (1986). *Acta Cryst.* A**40**, 140–149.

Sharma, A. K., Kumar, S. & Singh, T. P. (1999). *Acta Cryst.* D. Submitted.

Sharma, A. K., Paramasivam, M., Yadav, M. P., Srinivasan, A. & Singh, T. P. (1999). *J. Mol. Biol.* **289**, 303–317.

Sharma, A. K. & Singh, T. P. (1999). *Acta Cryst.* D**55**, 1799–1804.

Sharma, A. K., Rajashankar, K. R., Yadav, M. P. & Singh, T. P. (1999). *Acta Cryst.* D**55**, 1152–1157.

Smith, C. A., Anderson, B. F., Baker, H. M. & Baker, E. N. (1992). *Biochemistry*, **31**, 4527–4533.

Sthuchell, R. N., Farris, R. L. & Mandel, I. D. (1981). *Ophthalmology*, **88**, 858–861.